*American Mineralogist, Volume 94, pages 1071–1074, 2009*

**LETTER**

# Structure determination of the 2.5 hydrate $MgSO_4$ phase by simulated annealing

**HONGWEI MA,[1] DAVID L. BISH,[1,*] HSIU-WEN WANG,[1] AND STEVE J. CHIPERA[2]**

[1]Department of Geological Sciences, Indiana University, 1001 East 10th Street, Bloomington, Indiana 47405, U.S.A.
[2]Chesapeake Energy Corporation, 6100 N. Western Avenue, Oklahoma City, Oklahoma 73118, U.S.A.

## ABSTRACT

The crystal structure of the 2.5 hydrate $MgSO_4$ phase was determined by simulated annealing from laboratory X-ray powder diffraction data measured from 2–140 °2θ using Cu$K\alpha$ radiation. The 2.5 hydrate is monoclinic, space group $C2/c$, with unit-cell parameters $a$ = 18.8636(4) Å, $b$ = 12.3391(2) Å, $c$ = 8.9957(2) Å, β = 94.568(2)°, $V$ = 2087.1(6) Å$^3$, and $Z$ = 16. The model was refined using fundamental-parameters Rietveld refinement, converging to $R_{wp}$ = 8.89%, $R_p$ = 6.61%, $R_{exp}$ = 3.33%, $R_{Bragg}$ = 3.95%, and $\chi^2$ = 2.67. The refined structure is consistent with a formula of 2.5 $H_2O$. Bond-valence calculations for the refined model show that the structure is chemically sensible. In the refined structure, $[Mg(O,H_2O)_6]$ octahedra and $[SO_4]$ tetrahedra build up 2-D double-sheet slabs by sharing vertex O atoms, which are held together by inter-slab H-bonds involving $(SO_4)^{2-}$ groups and $H_2O$ molecules coordinated with $Mg^{2+}$ cations to form the layer structure of the 2.5 hydrate phase.

**Keywords:** $MgSO_4{\cdot}2.5H_2O$, $MgSO_4{\cdot}2.4H_2O$, crystal structure, simulated annealing, structure determination, powder diffraction, Rietveld refinement

## INTRODUCTION

Various hydrated magnesium sulfates, $MgSO_4{\cdot}nH_2O$, are stable over a wide range of temperature-humidity conditions on the surface of Earth, most of which have been identified/synthesized and structurally characterized, e.g., $n$ = 1 (kieserite; Aleksovska et al. 1998), $n$ = 2 (sanderite; Ma et al. 2009), $n$ = 4 (starkeyite; Baur 1964), $n$ = 5 (pentahydrite; Baur and Rolin 1972), $n$ = 6 (hexahydrite; Zalkin et al. 1964), $n$ = 7 (epsomite; Calleri et al. 1984), and $n$ = 11 (meridianiite; Peterson et al. 2007). At least since the time of the Mars Viking landers (Clark et al. 1976), magnesium sulfate hydrates have also been predicted to exist on the surface of Mars. This prediction was strengthened by chemical and spectroscopic data from recent missions (Bish et al. 2003; Feldman et al. 2003, 2004; Vaniman et al. 2004; Bibring et al. 2005; Gendrin et al. 2005; Chipera and Vaniman 2007; Mangold et al. 2008). The hydration states of magnesium sulfates and their distribution on the surface of Mars help to understand the history of water on this planet due to the sensitivity of hydrated magnesium sulfates to temperature and humidity. Knowledge of the crystal structures and stability relations for the $MgSO_4{\cdot}nH_2O$ series are necessary to infer which species can exist on the Martian surface and, if present, how much $H_2O$ they may contain, how the $H_2O$ is contained, and how stable the $H_2O$ molecules are in the structure. The stabilities of hydrated magnesium sulfate phases have been experimentally investigated recently under conditions similar to those on the surface of Mars (Chipera and Vaniman 2007), and several previously unknown phases were obtained. One of these, referred to as the "unknown phase," persisted through several experiments and appeared to contain ~2.4 $H_2O$. The structure of this phase is unknown and no crystallographic information is available in the International Center for Diffraction Data (ICDD) database. In this letter, we report the structure determination of this new hydrate of $MgSO_4$ from X-ray powder diffraction data measured on a synthetic sample.

## EXPERIMENTAL METHODS

The starting material for synthesis of the unknown phase was an ultra-pure $MgSO_4{\cdot}6H_2O$ reagent that is principally hexahydrite at the temperature ($T$) and relative humidity (RH) conditions in our laboratory (Alfa Aesar Puratronic 99.997%, CAS 22189-08-8). In accord with the approximate $T$-RH field in the $MgSO_4$-$H_2O$ stability diagram (Chipera and Vaniman 2007), the unknown phase was prepared by maintaining the starting materials in the appropriate $T$-RH region in an environmental cell on the X-ray diffractometer, bypassing the formation of other intermediate hydrates. The diffractometer heating stage and flat-plate sample were maintained at 75 °C, and a mixture of $H_2O$ and $N_2$ gas with 95% RH (at 23 °C) was generated and introduced into the environmental cell according to Chipera et al. (1997). The effective RH at 75 °C, ~14%, was calculated from the vapor pressure of $H_2O$ according to the Harr steam tables. These synthesis conditions were maintained during controlled-atmosphere X-ray diffraction (XRD) measurements (2–70 °2θ, 0.02° steps, 4 s/step) to monitor the progression of phases. As the $T$-RH conditions for the unknown phase are significantly outside the stability field for hexahydrite, the solid first transformed into an amorphous phase from which the unknown phase subsequently formed within 4–8 h. This same specimen was used to collect XRD data for structure determination (2–140 °2θ, 0.02° step size, 12 s/step), during which time the XRD heating stage and sample were maintained at 75 °C. All diffraction data were measured using a Siemens D500 diffractometer with Cu$K\alpha$ radiation, incident- and diffracted-beam Soller slits, and a Kevex PSi solid-state detector. The specimen used for structure solution was close to pure

*E-mail: bish@indiana.edu

2.5 hydrate, with ~2.3 wt% sanderite ($2H_2O$) and ~1.3 wt% hexahydrite ($6H_2O$) as determined by multicomponent Rietveld refinement after structure solution. The Lorentzian crystallite size and strain for the 2.5 hydrate are 474(28) nm and 0.18(1)%, respectively. No internal standard was used, so we were unable to determine the amount of any amorphous phase. It is relatively straightforward to detect small amounts of a crystalline component (with sharp peaks) by Rietveld refinement, but small amounts of amorphous components cannot be detected, as documented in the literature.

TGA analysis on a ~14 mg sample of the unknown phase used in XRD measurements gave a weight loss of ~26.4% from 23 to 400 °C, corresponding to ~2.4 $H_2O$ molecules/unit cell. The discrepancy between this value and the theoretical $H_2O$ content (2.5, see below) likely reflects admixture with a small amount (~9 wt%, which would not be detectable by XRD) of the amorphous hydrated $MgSO_4$ that contains ~17% $H_2O$. Both XRD and TGA measurements were repeated, giving substantially the same results.

## RESULTS AND DISCUSSION

### Unit cell, space group, and unit-cell contents

Twenty-four diffraction peaks below 35 °2θ were selected and indexed using the single-value decomposition method (Coelho 2003) implemented in TOPAS Academic 4.1 (Coelho 2007). The result was confirmed by indexing the pattern with DICVOL04 (Boultif and Louer 2004) and ITO (Visser 1969). Refined unit-cell parameters from DICVOL04 are: $a$ = 18.867(3) Å, $b$ = 12.340(2) Å, $c$ = 9.003(1) Å, α = 90°, β = 94.51(2)°, γ = 90°, with M(20) = 18.4, F(20) = 39.7 where M(20) and F(20) are the de Wolff figures of merit (de Wolff 1968) and the F index, respectively. This unit cell accounted for all the peaks in the pattern except the peak at 16.16 °2θ, which can be assigned to the hexahydrite ($1\ \bar{1}\ \bar{2}$) peak and the sanderite (111) peak. Diffraction intensities for each reflection in the range of 5–80° were obtained using Le Bail profile fitting (Le Bail et al. 1988) implemented in the program TOPAS, and the final $R_{wp}$ for the Le Bail fit was 7.54%. Observed extinction conditions were $hkl$: $h + k = 2n$; $h0l$: $l = 2n$. The possible space groups were thus determined to be either $Cc$ (no. 9) or $C2/c$ (no. 15). No efforts were made to determine whether there is an inversion center in the structure, and we tried the two possible space groups in solving the structure. Ultimately, the structure was determined in the centrosymmetric space group $C2/c$ (no. 15). Thermal analysis data show that the probable formula for the unknown phase is approximately $MgSO_4 \cdot 2.4H_2O$. Based on 16 $MgSO_4 \cdot 2.4H_2O$ "molecules" in the unit cell, the calculated density is 2.08 g/cm$^3$, consistent with measured and calculated densities in the $MgSO_4 \cdot nH_2O$ series. As the final structure solution is consistent with a formula containing 2.5 $H_2O$ molecules (rather than 2.4), we will refer to the unknown phase subsequently in the text as the 2.5 hydrate.

### Structure determination by simulated annealing

Over the last 30 years, structure determination from powder diffraction data (SDPD) (David et al. 2006) has progressed greatly and has become a powerful alternative when samples are available only as crystalline powders. In addition to direct methods and the heavy-atom method, real-space global optimization techniques such as simulated annealing (SA) and genetic algorithms (GA) have been successfully applied to SDPD. SA is a well-established global optimization method based on the thermodynamic process of annealing a high-temperature melt. It was adapted for SDPD by replacing the atoms in a high-temperature melt and the corresponding energy of the system with a set of variable structure parameters and the corresponding value of a figure-of-merit function (crystallographic $R$ function), respectively. By varying the structure parameters and lowering the $R$-factor, the global minimum that corresponds to the correct structure configuration can be located and the structure is thereby determined. Before running SA for SDPD on the 2.5 hydrate, we must know the species and number of independent atoms in the unit cell and set up an annealing temperature regime. As mentioned above, the 2.5 hydrate has 16 $MgSO_4 \cdot 2.5H_2O$ molecules in the unit cell and belongs to space group $C2/c$, whose general position multiplicity is 8. Based on this information, crystallographically independent atoms can be reasonably presumed to be two Mg, two ($SO_4$) groups, and five $H_2O$ molecules. The initial positions of all of these atoms (except H) were set to 0, 0, 0. The temperature regime macro AUTO(T) as implemented in TOPAS Academic 4.1 (Coelho 2007) with T = 10 was used as the annealing temperature regime for solving this structure. SA for SDPD is time consuming and has difficulties in solving apparently simple inorganic structures due to the topological uncertainties of these materials. Therefore, structural and non-structural constraints and restraints are typically applied to assist in obtaining the correct solution within an acceptable time by forcing the program to try chemically plausible structure models only. Non-structural parameters were determined during Le Bail fitting of the diffraction data without atomic coordinates. These parameters, including background, specimen displacement, and profile parameters using the Thomson-Hasting-Cox pseudo-Voigt (THCZ) profile function, were then fixed during the structure-solution process. Two types of structural constraints were applied, anti-bump penalties (Sheldrick 1985) and distance and angle restraints for the ($SO_4$) and the [$Mg(O,H_2O)_6$] groups. Anti-bump penalties were used to prevent Mg-O, Mg-Mg, Mg-S, S-O, S-S, and O-O from being too close to each other. Atoms were merged if the distance between two atoms was <0.6 Å. Chemical knowledge and literature data (Hawthorne et al. 2000) show that all magnesium sulfate phases consist of ($SO_4$) tetrahedra and [$Mg(O,H_2O)_6$] octahedra. Therefore, [$SO_4$] and [$Mg(O,H_2O)_6$] groups were forced to be regular polyhedra with reasonable bond lengths and angles by using angle and distance restraints based on the Leonard-Jones potential. SA runs were performed using diffraction data in the range of 5–80 °2θ. The solution was found within 598.6 s after 474 SA runs on a DELL Optiplex 755 PC with a 2.4 GHz Intel Core2 Quad CPU. The global best $R$-factor dropped from 0.249 to 0.195 and then to 0.157 within 8 more SA runs, suggesting location of the correct solution. The SA runs were then terminated manually based on the global best $R_{wp}$ and real-time crystal structure plot. All independent non-hydrogen atoms were located at chemical sensible positions, but no effort was made to determine the location of hydrogen atoms.

### Rietveld refinement and structure validation

The structure model from SA was refined using the fundamental-parameters Rietveld approach implemented in TOPAS-Academic (Coelho 2007). Fundamental profile parameters for this refinement were determined from known instrumental parameters. Rietveld refinement was performed using data in

the range of 6–140 °2θ. Two peaks in the region of 98.2~99.2 and 115.8~116.8 °2θ known to be from the sample holder were excluded. The background was modeled by a six-order Chebyshev polynomial. Scale factor, unit-cell parameters, and atomic coordinates were refined, and occupancy factors were fixed to unity. Atomic displacement factors were fixed for groups of similar atoms to typical values. Soft constraints were applied to the ($SO_4$) tetrahedra and Mg-O distances, and these constraints were used throughout refinement to avoid local minima and to obtain more precise structure parameters. Other refined parameters include specimen displacement, crystallite size and strain, and a spherical harmonics preferred orientation correction (Järvinen 1993). The final Rietveld refinement converged to $R_{wp}$ = 8.89% with $\chi^2$ = 2.67, and the results are shown in Table 1. Selected geometrical parameters, a plot of the final Rietveld fit (Appendix 1 and 2), and the crystallographic information file are deposited.[1] Bond-valence summations (Brown 1992) were calculated to evaluate the refined model, although contributions from H atoms could not be included. The calculated bond-valence sums for unique atoms (except O atoms of $H_2O$ molecules) in the unit cell are: Mg1 2.20, Mg2 2.11, S1 6.14, S2 6.07, O1 1.92, O2 1.89, O3 1.50, O4 1.90, O5 1.81, O6 1.87, O7 1.92, and O8 1.94, in agreement with the expected oxidation states of these elements in the structure except the oxidation state of O3, which is obviously lower than the expected value because contributions from hydrogen atoms were not included.

## Structure description and discussion

Crystallographically unique atoms in the unit cell include two $Mg^{2+}$ cations, two $(SO_4)^{2-}$ groups, and five $H_2O$ molecules. Thus, two $MgSO_4$ "molecules" share five $H_2O$ molecules, and the formula for this hydrate is thus determined to be $MgSO_4 \cdot 2.5H_2O$ from structure analysis, instead of $MgSO_4 \cdot \sim 2.4H_2O$ from thermal analysis. One $Mg^{2+}$ atom is coordinated by three $H_2O$ molecules and three O atoms from three $(SO_4)^{2-}$ groups, whereas the other $Mg^{2+}$ atom is coordinated by two $H_2O$ molecules and four O atoms from four $(SO_4)^{2-}$ groups. The two sulfate groups also have different environments: one ($SO_4$) group shares four corners with four $Mg^{2+}$ cations and the other shares three O atoms with three $Mg^{2+}$ cations. The free O atom forms hydrogen bonds with $H_2O$ molecules. As a result, $[Mg(O,H_2O)_6]$ octahedra and ($SO_4$) tetrahedra form two-dimensional double-sheet slabs nearly parallel to the *b-c* plane by sharing part of their polyhedral apices. The slab consists of two sheets composed of alternating corner-sharing ($SO_4$) tetrahedra and $[Mg(O,H_2O)_6]$ octahedra. The slabs are then held together by H-bonds involving the free polyhedral vertices, building up the two-dimensional layer structure of the 2.5 hydrate (Fig. 1). As shown in Table 1, the average Mg-O distance is 2.05 Å, the average Mg-$H_2O$ length is slightly longer, with an average value of 2.09 Å, and the average S-O distance in the $(SO_4)^{2-}$ group is 1.47 Å. These values are in agreement with literature data for other $MgSO_4 \cdot nH_2O$ phases and those in other sulfate minerals in general (Hawthorne et al. 2000). Bond angles (see supporting materials) indicate that $[Mg(O,H_2O)_6]$ octahedra are distorted, whereas the ($SO_4$) tetrahedra deviate only slightly from ideal geometry.

All structures of the $MgSO_4 \cdot nH_2O$ system consist of ($SO_4$) tetrahedra and $[Mg(O,H_2O)_6]$ octahedra, and the linkage of polyhedra varies with the number of $H_2O$ molecules coordinated to $Mg^{2+}$ cations because $H_2O$ molecules coordinated with $Mg^{2+}$ cations usually do not bridge $[Mg(O,H_2O)_6]$ polyhedra (except kieserite). In the known structures of the $MgSO_4 \cdot nH_2O$ series, $Mg^{2+}$ can coordinate with two ($n$ = 1, 2), four ($n$ = 4, 5), or six ($n$ = 6, 7, 11) $H_2O$ molecules, and ($SO_4$) groups share four ($n$ = 1,2), two ($n$ = 4,5), or zero ($n$ = 6,7,11) apices with Mg-octahedra. As shown in the 2.5 hydrate, $Mg^{2+}$ can also be coordinated by three $H_2O$ molecules and ($SO_4$) groups shares three apices with Mg-octahedra. The structure of the 2.5 hydrate is the first two-dimensional layer structure in the $MgSO_4 \cdot nH_2O$ series. As discussed by Ma et al. (2009), the direct linkage of octahedra and tetrahedra of the $MgSO_4 \cdot nH_2O$ series decreases with increasing number of $H_2O$ molecules. This conclusion is verified by the layer structure of the 2.5 hydrate ($n$ = 2.5) that bridges the three-dimensional framework structures ($n$ = 1, 2) and the one-dimensional infinite chain structure ($n$ = 5). Building blocks of all low-dimension structures in $MgSO_4 \cdot nH_2O$ hydrates, such as

**Table 1.** Atomic coordinates, equivalent isotropic displacement parameters (Å²), and selected bond lengths (Å) for $MgSO_4 \cdot 2.5H_2O$

| Atom | x | y | z | $B_{eq}$ |
|---|---|---|---|---|
| Mg1 | 0.3663(1) | 0.6193(2) | 0.4811(3) | 0.8 |
| Mg2 | 0.3977(1) | 0.1199(2) | 0.4053(3) | 0.8 |
| S1 | 0.3361(1) | 0.3743(2) | 0.3426(3) | 0.4 |
| S2 | 0.5733(1) | 0.1307(2) | 0.4527(3) | 0.4 |
| O1 | 0.3590(4) | 0.4565(3) | 0.4505(7) | 1.2 |
| O2 | 0.3332(3) | 0.4139(7) | 0.1879(4) | 1.2 |
| O3 | 0.2654(2) | 0.3307(7) | 0.3691(9) | 1.2 |
| O4 | 0.3839(4) | 0.2801(3) | 0.3520(8) | 1.2 |
| O5 | 0.6258(3) | 0.2157(3) | 0.5059(9) | 1.2 |
| O6 | 0.5012(2) | 0.1762(6) | 0.4458(9) | 1.2 |
| O7 | 0.5814(4) | 0.0429(3) | 0.5619(7) | 1.2 |
| O8 | 0.5897(4) | 0.0789(5) | 0.3144(4) | 1.2 |
| O1w | 0.4736(2) | 0.6027(6) | 0.5573(9) | 1.5 |
| O2w | 0.3919(5) | 0.6347(7) | 0.2593(5) | 1.5 |
| O3w | 0.2592(2) | 0.6438(7) | 0.4233(4) | 1.5 |
| O4w | 0.2882(2) | 0.0798(7) | 0.3748(9) | 1.5 |
| O4w | 0.3843(4) | 0.1497(6) | 0.6302(5) | 1.5 |

| | | | | | | | |
|---|---|---|---|---|---|---|---|
| Mg1-O1 | 2.029(5) | Mg2-O4 | 2.046(5) | S1-O1 | 1.446(6) | S2-O5 | 1.494(7) |
| Mg1-O2* | 2.049(6) | Mg2-O6 | 2.079(5) | S1-O2 | 1.471(6) | S2-O6 | 1.469(6) |
| Mg1-O5† | 2.043(5) | Mg2-O7‡ | 2.064(5) | S1-O3 | 1.473(7) | S2-O7 | 1.462(6) |
| Mg1-O1w | 2.094(6) | Mg2-O8§ | 2.071(5) | S1-O4 | 1.469(6) | S2-O8 | 1.454(6) |
| Mg1-O2w | 2.098(6) | Mg2-O4w | 2.120(6) | | | | |
| Mg1-O3w | 2.067(6) | Mg2-O5w | 2.091(6) | | | | |

*Note:* Symmetry transformations used to generate equivalent atoms: * *x*, 1 – *y*, 0.5 + *z*; † 1 – *x*, 1 – *y*, 1 – *z*; ‡ 1 – *x*, –*y*, 1 – *z*; § 1 – *x*, *y*, 0.5 – *z*.

[1] Deposit item AM-09-035, Appendix Figure, Table, and CIF. Deposit items are available two ways: For a paper copy contact the Business Office of the Mineralogical Society of America (see inside front cover of recent issue) for price information. For an electronic copy visit the MSA web site at http://www.minsocam.org, go to the American Mineralogist Contents, find the table of contents for the specific volume/issue wanted, and then click on the deposit link there.

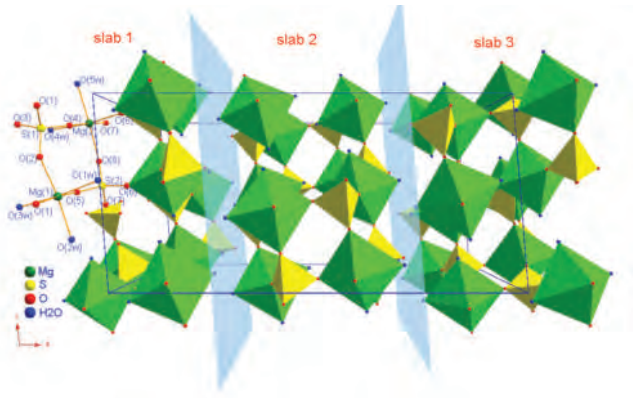


**FIGURE 1.** Crystal structure of $MgSO_4 \cdot 2.5H_2O$.

starkeyite, pentahydrite, hexahydrite, epsomite, and meridianiite, are held together by H-bonds. Similarly, slabs in the 2.5 hydrate link in the [100] direction through H-bonds involving ($SO_4$) and [$Mg(O,H_2O)_6$] between adjacent layers. Atoms within the slabs are bonded together by strong chemical interactions, and there are no $H_2O$ molecules between the slabs. This structural feature is consistent with the experimental result that the 2.5 hydrate persists under varied experimental conditions of temperature and relative humidity, in contrast to many layer-structure materials that are extremely sensitive to changes in temperature and relative humidity.

## ACKNOWLEDGMENTS

This research was funded in part by a NASA Mars Fundamental Research grant, no. NNG06GH40G, to D.L.B.

## REFERENCES CITED

Aleksovska, S., Petrusevski, V.M., and Soptrajanov, B. (1998) Calculation of structural parameters in isostructural series: the kieserite group. Acta Crystallographica, B54, 564–567.

Baur, W.H. (1964) On the crystal chemistry of salt hydrates. II. A neutron diffraction study of $MgSO_4.4H_2O$. Acta Crystallographica, 17, 863–869.

Baur, W.H. and Rolin, J.L. (1972) Salt hydrates. IX. The comparison of the crystal structure of magnesium sulfate pentahydrate with copper sulfate pentahydrate and magnesium chromate pentahydrate. Acta Crystallographica, 28, 1448–1455.

Bibring, J.-P., Langevin, Y., Gendrin, A., Gondet, B., Poulet, F., Berthe, M., Soufflot, A., Arvidson, R., Mangold, N., Mustard, J., Drossart, P., and the OMEGA Team (2005) Mars surface diversity as revealed by the OMEGA/Mars Express observations. Science, 307, 1576–1581.

Bish, D.L., Carey, J.W., Vaniman, D.T., and Chipera, S.J. (2003) Stability of hydrous minerals on the martian surface. Icarus, 164, 96–103.

Boultif, A. and Louer, D. (2004) Powder pattern indexing with dichotomy method. Journal of Applied Crystallography, 37, 724–731.

Brown, I.D. (1992) Chemical and steric constraints in inorganic solids. Acta Crystallographica, B48, 553–572.

Calleri, M., Gavetti, A., Ivaldi, G., and Rubbo, M. (1984) Synthetic epsomite, $MgSO_4 \cdot 7H_2O$: absolute configuration and surface features of the complementary {111} forms. Acta Crystallographica, B40, 218–222.

Chipera, S.J. and Vaniman, D.T. (2007) Experimental stability of magnesium sulfate hydrates that may be present on Mars. Geochimica et Cosmochimica Acta, 71, 241–250.

Chipera, S.J., Carey, J.W., and Bish, D.L. (1997) Controlled-humidity XRD analyses: Application to the study of smectite expansion/contraction. In J.V. Gilfrich, I.C. Noyan, R. Jenkins, T.C. Huang, R.L. Snyder, D.K. Smith, M.A. Zaitz, and P.K. Predecki, Eds., Advances in X-Ray Analysis, 39, p. 713–722. Plenum Press, New York.

Clark, B.C., Baird, A.K., Rose Jr., H.J., Toulmin III, P., Keil, K., Castro, A.J., Kelliher, W.C., Rowe, C.D., and Evans, P.H. (1976) Inorganic analysis of martian surface samples at the Viking landing sites. Science, 194, 1283–1288.

Coelho, A.A. (2003) Indexing of powder diffraction patterns by iterative use of singular value decomposition. Journal of Applied Crystallography, 36, 86–95.

——— (2007) TOPAS Academic 4.1 Technical reference, http://members.optusnet.com.au/alancoelho.

David, W.I.F., Shankland, K., McCusker, L.B., and Baerlocher, Ch. (2006) Structure Determination from Powder Diffraction Data, p. 252–285. Oxford University Press, U.K.

de Wolff, P.M. (1968) A simplified criterion for the reliability of a powder pattern indexing. Journal of Applied Crystallography, 1, 108–113.

Feldman, W.C., Prettyman, T.H., Maurice, S., Plaut, J.J., Bish, D.L., Vaniman, D.T., Mellon, M.T., Metzger, A.E., Squyres, S.W., Karunatillake, S., Boynton, W.V., Elphic, R.C., Funsten, H.O., Lawrence, D.J., and Tokar, R.L. (2003) Global distribution of near-surface hydrogen on Mars. Journal of Geophysical Research, 109, E09006.

Feldman, W.C., Mellon, M.T., Maurice, S., Prettyman, T.H., Carey, J.W., Vaniman, D.T., Bish, D.L., Fialips, C.I., Chipera, S.J., Kargel, J.S., Elphic, R.C., Funsten, H.O., Lawrence, D.J., and Tokar, R.L. (2004) Hydrated states of $MgSO_4$ at equatorial latitudes on Mars. Geophysical Research Letters, 31, L16702.

Gendrin, A., Mangold, N., Bibring, J.-P., Langevin, Y., Gondet, B., Poulet, F., Bonello, G., Quantin, C., Mustard, J., Arvidson, R., and LeMouelic, S. (2005) Sulfates in martian layered terrains: The OMEGA/Mars Express view. Science, 307, 1587–1591.

Hawthorne, F.C., Krivovichev, S.V., and Burns, P.C. (2000) The crystal chemistry of sulfate minerals. In C.N. Alpers, J.L. Jambor, and D.K. Nordstrom, Eds., Sulfate Minerals: Crystallography, Geochemistry and Environmental Significance, 40, p. 1–101. Reviews in Mineralogy and Geochemistry, Mineralogical Society of America, Chantilly, Virginia.

Järvinen, M. (1993) Application of symmetrized harmonics expansion to correction of the preferred orientation effect. Journal of Applied Crystallography, 26, 525–531.

Le Bail, A., Duroy, H., and Fourquet, J.L. (1988) Ab initio structure determination of $LiSbWO_6$ by X-ray powder diffraction. Materials Research Bulletin, 23, 447–452.

Ma, H.W., Bish, D.L., Wang, H.W., and Chipera, S.J. (2009) Determination of the crystal structure of sanderite, $MgSO_4 \cdot 2H_2O$, by X-ray powder diffraction and the charge-flipping method. American Mineralogist, 94, 622–625.

Mangold, N., Gendrin, A., Gondet, B., LeMouelic, S., Quantin, C., Ansan, V., Bibring, J.-P., Langevin, Y., Masson, P., and Neukum, G. (2008) Spectral and geological study of the sulfate-rich region of West Candor Chasma, Mars. Icarus, 194, 519–543.

Peterson, R.C., Nelson, W., Madu, B., and Shurvell, H.F. (2007) Meridianiite: A new mineral species observed on Earth and predicted to exist on Mars. American Mineralogist, 92, 1756–1759.

Sheldrick, G.M. (1985) SHELX86. Program for the solution of crystal structures. University of Gottingen, Germany.

Vaniman, D.T., Bish, D.L., Chipera, S.J., Fialips, C.I., Carey, J.W., and Feldman, W.C. (2004) Magnesium sulfate salts and the history of water on Mars. Nature, 431, 663–665.

Visser, J.W. (1969) A fully automatic program for finding the unit cell from powder data. Journal of Applied Crystallography, 2, 89–95.

Zalkin, A., Ruben, H., and Templeton, D.H. (1964) The crystal structure and hydrogen bonding of magnesium sulfate hexahydrate. Acta Crystallographica, 17, 235–240.

MANUSCRIPT RECEIVED FEBRUARY 18, 2009
MANUSCRIPT ACCEPTED APRIL 8, 2009
MANUSCRIPT HANDLED BY BRYAN CHAKOUMAKOS